Intrinsic electronic switching time in ultrathin epitaxial vanadium dioxide thin film

Ayan Kar, Nikhil Shukla, Eugene Freeman, Hanjong Paik, Huichu Liu, Roman Engel-Herbert, S. S. N. Bharadwaja, Darrell G. Schlom, and Suman Datta

Citation: Applied Physics Letters **102**, 072106 (2013); doi: 10.1063/1.4793537
View online: http://dx.doi.org/10.1063/1.4793537
View Table of Contents: http://scitation.aip.org/content/aip/journal/apl/102/7?ver=pdfcov
Published by the AIP Publishing

Articles you may be interested in
Optical switching and photoluminescence in erbium-implanted vanadium dioxide thin films
J. Appl. Phys. **115**, 093107 (2014); 10.1063/1.4867481

Publisher's Note: “Intrinsic electronic switching time in ultrathin epitaxial vanadium dioxide thin film” [Appl. Phys. Lett. 102, 072106 (2013)]
Appl. Phys. Lett. **103**, 129904 (2013); 10.1063/1.4821744

Epitaxial growth and metal-insulator transition of vanadium oxide thin films with controllable phases
Appl. Phys. Lett. **101**, 071902 (2012); 10.1063/1.4745843

Enhanced performance of room-temperature-grown epitaxial thin films of vanadium dioxide
Appl. Phys. Lett. **98**, 251916 (2011); 10.1063/1.3600333

Effect of the substrate on the insulator–metal transition of vanadium dioxide films
J. Appl. Phys. **109**, 063708 (2011); 10.1063/1.3563588

Want to publish your paper in the
#1 MOST CITED journal in applied physics?
With Applied Physics Letters, you can.
AIP | Applied Physics Letters
THERE'S POWER IN NUMBERS. Reach the world with AIP Publishing.

This article is copyrighted as indicated in the article. Reuse of AIP content is subject to the terms at: http://scitation.aip.org/termsconditions. Downloaded to IP: 128.84.143.26 On: Mon, 27 Apr 2015 13:54:41

Intrinsic electronic switching time in ultrathin epitaxial vanadium dioxide thin film

Ayan Kar,[1,a)] Nikhil Shukla,[1] Eugene Freeman,[1] Hanjong Paik,[2] Huichu Liu,[1] Roman Engel-Herbert,[3] S. S. N. Bharadwaja,[3] Darrell G. Schlom,[2] and Suman Datta[1]
[1]*Department of Electrical Engineering, The Pennsylvania State University, University Park, Pennsylvania 16802, USA*
[2]*Department of Materials Science and Engineering, Cornell University, Ithaca, New York 14853, USA*
[3]*Department of Materials Science and Engineering, The Pennsylvania State University, University Park, Pennsylvania 16802, USA*

(Received 21 November 2012; accepted 12 February 2013; published online 22 February 2013; corrected 28 August 2013)

This letter investigates the intrinsic electronic switching time associated with the insulator-to-metal phase transition in epitaxial single crystal vanadium dioxide (VO_2) thin films using impedance spectroscopy and ac conductivity measurements. The existence of insulating and metallic phase coexistence, intrinsic to the epitaxial (001) oriented VO_2 thin film grown on a (001) rutile TiO_2 substrate, results in a finite capacitance being associated with the VO_2 films in their insulating phase that limits the electronic switching speed. Insights into the switching characteristics and their correlation to the transport mechanism in the light of phase coexistence are obtained by performing a detailed scaling study on VO_2 two-terminal devices. © *2013 American Institute of Physics*.
[http://dx.doi.org/10.1063/1.4793537]

Vanadium dioxide (VO_2) is a correlated electron material that exhibits an insulator-to-metal phase transition (IMT). VO_2 thin films have demonstrated an abrupt transition with up to 4 orders of magnitude change in resistivity;[1] in single crystals, this is up to 5 orders of magnitude.[2] This paves the way for its potential application in steep slope electronic switching devices or memory elements. To realize practical implementation of VO_2 based metal-to-insulator phase transition (MIT) devices, systematic studies on electronic switching characteristics need to be understood. Further, continued scaling is required to reduce the dynamic power consumption and enhance the switching speed, which could ultimately lead to the realization of useful abrupt switching devices. To date, no detailed systematic investigation into the switching characteristics of VO_2,[3–5] as a function of dimensional scaling, has been done wherein the effects of metal-VO_2 interface and domain capacitances have been deconvoluted. In this letter, the electronic switching phenomenon in epitaxial VO_2 thin films is evaluated experimentally using pulsed current-voltage (I-V) and frequency dependent impedance spectroscopic measurements.[6]

Epitaxial VO_2 thin film of 10 nm thickness was grown directly on 0.5 mm thick (001) TiO_2 substrates via reactive oxide molecular beam epitaxy (MBE) system (Veeco GEN10). Details of the MBE growth and structural characterization of the epitaxial VO_2 films may be found elsewhere.[7] High-resolution transmission electron microscopy (HRTEM) analysis of the epitaxially grown VO_2 films was accomplished using a JEOL 2010F microscope. Two terminal VO_2 devices were fabricated using e-beam lithography starting with a dual layer of poly(methyl methacrylate)/methyl methacrylate (PMMA/MMA) resist stack to enable lift off patterning of Pd/Au, deposited by e-beam evaporation. The Pd/Au electrodes served as the anode and the cathode for two terminal characterization of VO_2 thin films. Subsequently, VO_2 channels for individual devices were patterned using a negative e-beam resist (NEB-31) and a CF_4 based dry etch process. Finally, the resist was stripped off using Remover 1165 at 70 °C for 30 min followed by a 10 min sonication at room temperature. The scanning electron microscopic image of the resultant two terminal VO_2 device is shown in Fig. 1(a). The pulsed I-V experiments were done using an Agilent 81150A arbitrary waveform generator and an Agilent DSO9104A oscilloscope in 1 MΩ impedance mode. Impedance spectroscopy measurements were done using an Agilent 4294A impedance analyzer, and an Agilent 4285A LCR-meter was used to measure the AC conductivity.

The change in the phase of VO_2 was observed by measuring the potential drop across a load resistor in the circuit as shown in Fig. 1(b). Figure 2(a) shows the response of a 1 μm long channel device under test (DUT) for an input triangular voltage pulse having an amplitude and offset of 7.5 V and 0.5 V, respectively, with the corresponding voltage drop across a 3.3 kΩ load resistor (R_L and is parallel to 1 MΩ input impedance of oscilloscope-R_{Scope}) in series with the DUT. Triangular pulses were chosen to make sure that the device turn ON and turn OFF were explicitly observable under the triangular pulse as seen in Fig. 2(a). Turn ON refers to the forward mode phase switching from the insulating to the metallic state, and turn OFF refers to the reverse mode switching from the metallic state. An offset in the supply voltage was used to confirm that the device in the metallic state switched back to the insulating state (turned OFF) at a finite bias instead of following the trailing edge of the supply pulse without transitioning. This confirms that the MIT is electronically reversible. The switching time is extracted by extrapolating to zero load resistance $R_L = 0$ Ω. The extrapolated rise (t_{rise}) and fall (t_{fall}) time for a device with 1 μm long VO_2 channel was estimated to be 118 ns and 55 ns, respectively, as seen in Fig. 2(b). Further, using the

[a)]auk33@psu.edu.

 © 2013 American Institute of Physics

This article is copyrighted as indicated in the article. Reuse of AIP content is subject to the terms at: http://scitation.aip.org/termsconditions. Downloaded to IP: 128.84.143.26 On: Mon, 27 Apr 2015 13:54:41

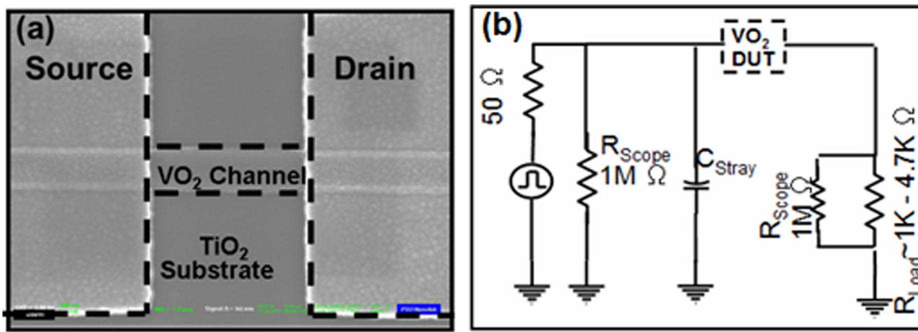

FIG. 1. (a) SEM image of VO_2 two terminal device used in switching experiment. (b) Equivalent circuit model of pulsed IV experimental setup.

equivalent circuit model shown in Fig. 1(b) and modelling the VO_2 device as a variable resistor and constant parallel capacitor (0.512 pF), as extracted in 5(a)), we simulate the IMT and MIT in the device as seen in Figs. 2(c)–2(f), where V_{SUPPLY} from the experiment was used as the source. Figure 2(f) shows a close match between the H-spice circuit simulation and the experimental results obtained from the voltage drop across the 3.3 K load (V_{LOAD}).

The extraction of intrinsic switching time from pulsed I-V measurements holds true only if the VO_2 film is considered as a lumped resistor and capacitor. We, however, explore the possibility of internal bulk capacitance serving as a limitation to the switching time due to charging/discharging effects. In the insulating state, VO_2 may be electrically represented as an equivalent R-C parallel network. Frequency domain impedance spectroscopy (IS) measurements were performed on a 10 nm thick and 1 μm long VO_2 channel with the VO_2 film in its insulating state by applying a 500mV_{rms} ac signal (100 Hz–10 MHz). Figure 3(a) shows the Cole-Cole plots ($-$Im(Z) vs Re(Z)) obtained for the device structure. Experimental data were modelled as a R-C_{CPE} network having an impedance of $Z = R + 1/[(j\omega)^n C_m]$. The depressed nature of the experimental Cole-Cole plot with respect to that simulated by modelling VO_2 as an ideal R-C network indicates a non-ideal capacitance arising due to non-ideal Debye relaxation processes.[8] This non-ideal capacitance of VO_2 can be modelled as a constant phase element (CPE) given as $C_{CPE} = C_m(\omega)^{n-1}$ where the non-ideality factor $n \in [0, 1]$ is a measure of the inhomogenity in the film.[9] Modelling of the impedance spectrum of VO_2 as an equivalent R-C_{CPE} network is shown in Fig. 3(a). From this, we extract an intrinsic equivalent resistance (R_{eq}) = 5.69 MΩ and capacitance (C_{CPE}) = 0.512 pF with a non-ideality factor of n = 0.8 associated with the capacitance of the circuit. Further, the impedance data were represented using $Z''(= \text{Imag}(Z))$ vs. frequency and M'' $(= j\omega CZ^*)$ vs. frequency plots shown in Fig. 3(b). The Z'' plot helps to identify the most resistive element while the M'' plot picks out the smallest capacitance associated with the structure.[6] The absence of multiple peaks in the M'' plot vs. frequency in Fig. 3(b) indicates the presence of a single capacitive component which could plausibly arise from the metal-VO_2 interface or multiple indistinguishable R-C components arising from the presence of short range domains within VO_2 thin film.

To ascertain the nature of the capacitive response, the complex impedance response on VO_2 devices with different channel lengths varying from 0.5 μm to 10 μm (width is kept constant at 2 μm) are measured as shown in Fig. 4(a). The

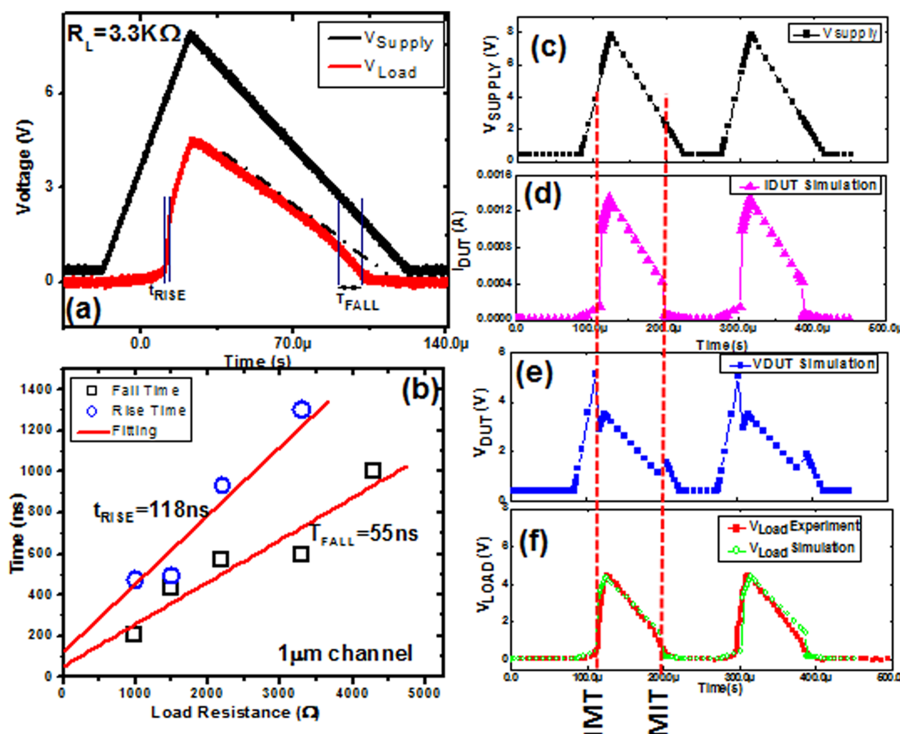

FIG. 2. (a) Triangular V_{Supply} pulse and corresponding potential drop V_{Load} across a 3.3 kΩ load resistor. (b) Rise and fall times for various load resistor extrapolated to extract VO_2 switching times. Equivalent circuit model in Figure 1(b) was used for H-spice switching simulation of the (d) voltage drop across the DUT (V_{DUT}), (e) current flowing through the circuit (I_{DUT}), and (f) voltage drop across the 3.3 K load resistor (V_{Load}) compared with the experimental data from (a).

This article is copyrighted as indicated in the article. Reuse of AIP content is subject to the terms at: http://scitation.aip.org/termsconditions. Downloaded to IP: 128.84.143.26 On: Mon, 27 Apr 2015 13:54:41

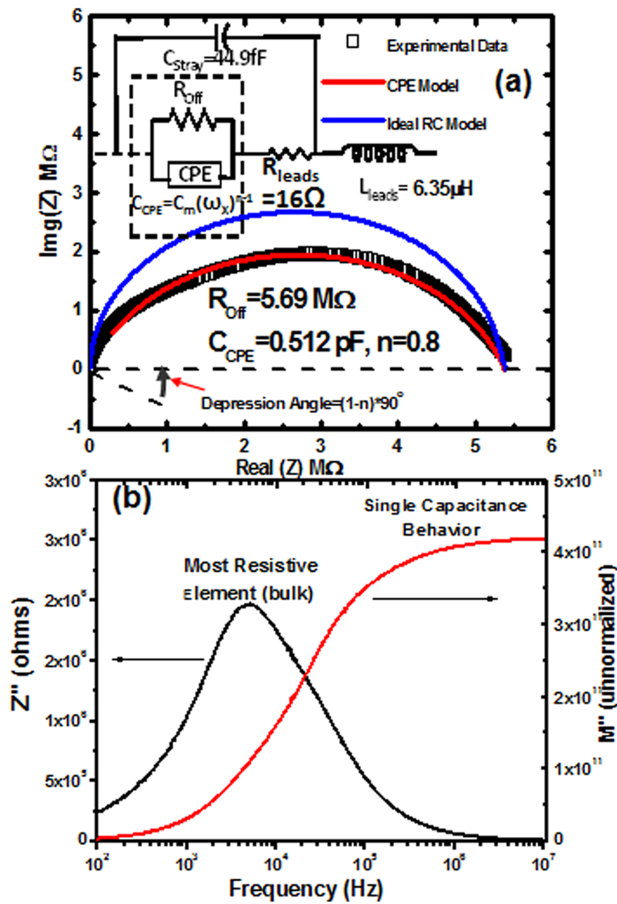

FIG. 3. (a) Cole-Cole plot from impedance spectroscopy obtained from a 10 nm thin and 1 μm long VO_2 channel by applying a 500 mV AC small signal (100 Hz–10 MHz). Experimental plot, which was modelled as an equivalent R-C_{CPE} network ($Z = R + 1/[(j\omega)^n C_m]$), shows depressed nature of the plot. (b) The impedance data from (a) represented using $Z''(= \mathrm{Imag}(Z))$ v/s frequency and M'' ($= j\omega CZ^*$) v/s frequency plots.

variation of the R_{eq} and the normalized C_{eq} ($=$C/A, normalized to contact area $= 2500\,\mu m^2$) are shown in Fig. 4(b). The equivalent resistance (R_{eq}) scales linearly with channel length and the normalized capacitance (C_{eq}) vs channel length response indicates that the capacitance response is due to the intrinsic nature of bulk VO_2 (insulator state) rather than the metal-VO_2 interface.[9] This points to the presence of multiple indistinguishable R-C networks each associated with a domain boundary within the VO_2 bulk since considering VO_2 as a pure dielectric (without any short range order domains) would result in a geometrical capacitance of $\sim$1–10 aF. The presence of domains in the MBE grown epitaxial single crystalline VO_2 film is corroborated by the cross-sectional HRTEM images as shown in Fig. 4(c). Figure 4(d) shows the scaling of the RC time constant ($t_{RC} = R*C$), with the channel length (L) where a $t_{RC} \propto L^2$ dependence is observed. When VO_2 is switched electrically, t_{RC} is a critical component of the total switching time. The multiple indistinguishable R-C networks associated with the domains, mentioned earlier, undergo electronic charging, the time scale for which is decided by t_{RC}. When the carrier density exceeds the Mott criterion, $n > n_{mott}$, the Columbic repulsion "U" gets screened thereby favouring transition to the metallic state and eliminating the capacitance associated with the domain wall.

The evolution of the VO_2 film characteristics as we drive it across the IMT has been studied using temperature dependent IS shown in Figs. 5(a) and 5(b). In the insulating state (Fig. 5(a)), as the temperature increases, the capacitance increases while the resistance of the 500 nm long and 10 nm thin VO_2 channel is observed to decrease as plotted in Fig. 5(c). Across the transition, the equivalent circuit for the metallic VO_2 film can be represented as a series R-L network (shown in the inset of Fig. 5(b)) where $L \sim 3.6\,\mu H$. This

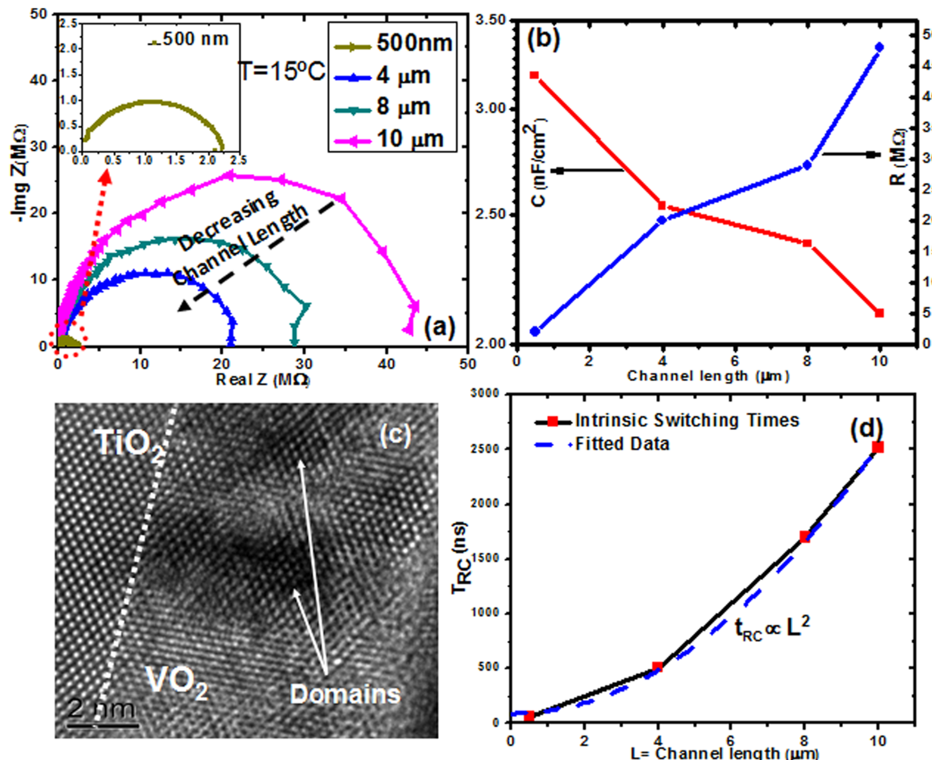

FIG. 4. (a) Cole-Cole plots from impedance spectroscopy obtained from devices with VO_2 channel lengths varying from 0.5 μm to 10μm (width kept constant at 2 μm). (b) Extracted R and C values from the IS data in (a). (c) HRTEM cross-sectional image of epitaxially grown crystalline VO_2 film (10 nm) on TiO_2 substrate. (d) t_{RC} plotted for various channel lengths.

This article is copyrighted as indicated in the article. Reuse of AIP content is subject to the terms at: http://scitation.aip.org/termsconditions. Downloaded to IP: 128.84.143.26 On: Mon, 27 Apr 2015 13:54:41

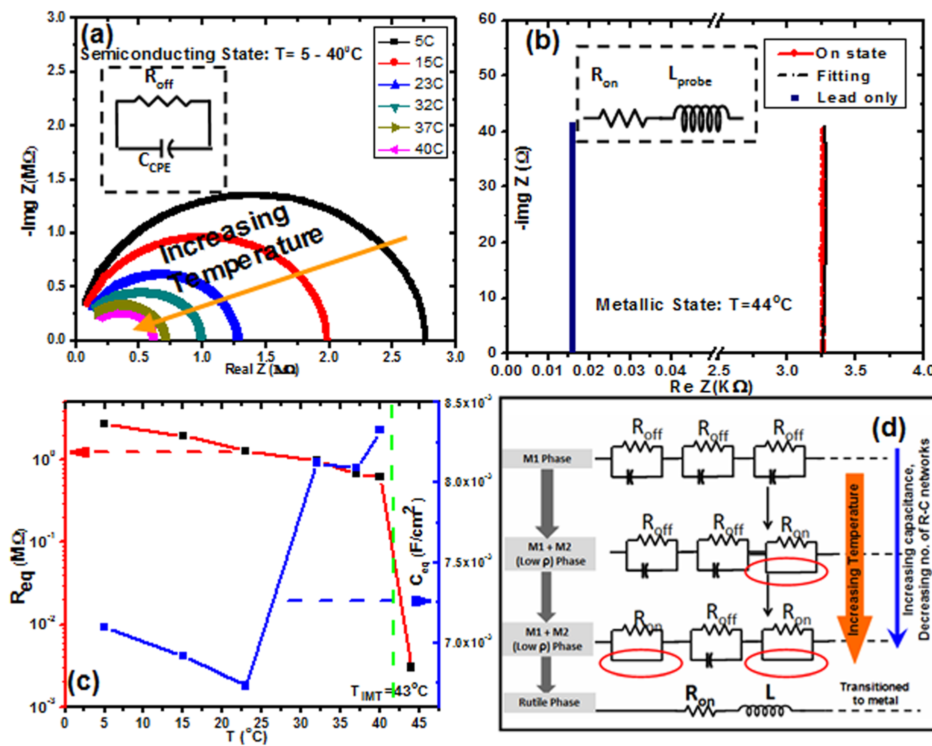

FIG. 5. (a) Temperature dependent impedance spectroscopy where the insulating VO_2 is modelled as an equivalent R-C_{CPE} network. (b) Post IMT impedance spectroscopy at 44 °C of metallic VO_2 represented as a R-L model. (c) Extracted R_{eq} and normalized C_{eq} values from IS as a function of temperature. (d) Schematic showing evolution of R-C networks and phase coexistence in VO_2 bulk to R-L networks across the IMT.

behaviour across the IMT phase boundary can also be understood in terms of the multiple indistinguishable R-C networks (also verified in the M″ plot in Fig. 3(b)) that characterize the VO_2 film in the insulating state. As the temperature increases, some of the insulating domains, which are in the monoclinic M1 phase, transition to an intermediate strongly correlated metallic M2 phase, which is characterized by a structure not too different from the M1 phase.[10] In terms of the electrical equivalent circuit, this phase transition can be modelled by a shunting of the capacitor associated with that R-C network of the insulating domain thereby eliminating its effective capacitive contribution, while R_{Off} changes to R_{On} as shown in Fig. 5(d). This explains why effective R reduces and C increases (in a series network, $C_{eq} = C_n/n$) with temperature. Simultaneously, the increasing number of M2 domains is consumed to form the rutile metallic phase as the VO_2 film transitions.[11] It is postulated that electron-phonon coupling close to the transition temperature T_C forms a polaron and as the polaron traverses through the lattice it leads to an ionic displacement of the V^+ ion annihilating the dimerization in the monoclinic phase thereby triggering a structural change (Peierls transition) into the rutile phase.

Further investigations of the VO_2 phase transition was accomplished using temperature dependent ac conductivity measurements as shown in Fig. 6(a). The measured total conductivity σ is given by the sum of the frequency independent band conductivity σ_{DC} and the frequency dependent AC conductivity $\sigma(\omega) \approx \omega^\beta$, where $\beta < 1$ is a signature of transport due to electron hopping in disordered systems.[12,13] Initially, far away from the transition temperature T_C, VO_2 is in the insulating state characterized by the M1 (Monoclinic) phase, where the conduction is dominated by hopping transport between the defect states in the 0.6 eV pseudo gap.[14] As explained before, the increasing temperature will switch some of the M1 domains into in an intermediate phase M2 (strongly correlated metal).[10] We speculate that transport in the M2 phase is dominated by band conduction and therefore

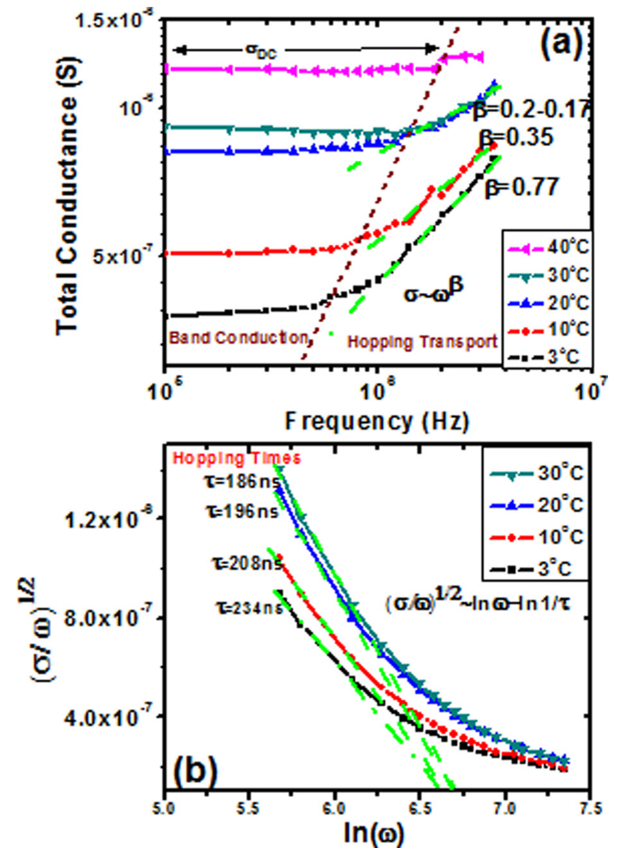

FIG. 6. (a) Total conductivity σ as a function of frequency (75 KHz–3.5 MHz) for various temperatures (3 °C–40 °C) with VO_2 in the insulating state. (b) Relaxation times τ extracted from the AC conductivity plot in (a) as a as a function of temperature.

This article is copyrighted as indicated in the article. Reuse of AIP content is subject to the terms at: http://scitation.aip.org/termsconditions. Downloaded to IP: 128.84.143.26 On: Mon, 27 Apr 2015 13:54:41

the net contribution of band transport is enhanced as the temperature rises and the density of M2 domains increase. This mechanism explains the phase coexistence in VO_2 (presence of conductive M2 phase domains in the insulating M1 phase below T_C) which accounts for the hopping transport (due to M1) and band transport (due to M2) in the system at temperatures below the Tc. This is further supported by the observation that the corner frequency increases with temperature as we approach the IMT which implies an increasing contribution of frequency independent dc band transport (Fig. 6(a)). As the pseudo gap collapses beyond the transition temperature, determined to be $\sim$45 °C, no frequency dependence is observed in the conductivity indicating that transport in the metallic regime is dominated by frequency independent band conduction in the *d* band. Based on the "pair model," the contribution of hopping transport (between a pair of localized levels) to the ac conductivity is given as $\sigma(\omega) \approx \omega \mathrm{Log}^2(1/\omega\tau)$, where τ is the hopping/relaxation time.[12] Fig. 6(b) shows τ as a function of temperature extracted from the ac conductivity plot in Fig. 6(a). It is, however, important to note that these extracted hopping times which are in the range of hundreds of nanoseconds do not fundamentally limit the electronic switching time of VO_2 film as extracted through IS measurements, since the transport processes near the VO_2 transition are governed by dc band conduction processes.

In this letter, we provide a detailed investigation of electronic switching characteristics of VO_2 thin films as a function of the device channel length. Extrapolated switching times obtained from pulsed IV measurements alone do not reveal the true switching time of the device. Impedance spectroscopy reveals that VO_2 in the insulating state cannot be represented as a simple lumped resistor. HRTEM cross-sectional images of epitaxial VO_2 films reveal the presence of VO_2 domains in the VO_2 bulk and each of which can be represented as an R-C network as confirmed by temperature dependent impedance spectroscopy analysis as a function of device size. This internal bulk capacitance fundamentally limits the electronic switching speed of the device. AC conductivity measurements reveal that hopping and dc band conduction transport mechanisms contribute to the total conductivity in the insulating state and the relative contribution of the latter mechanism increases as we approach the transition temperature. Therefore, the relaxation times associated with hopping transport, which dominate at lower temperatures, do not fundamentally control the IMT switching time.

The authors would like to thank Professor Srinivas Tadigadapa for use of his Impedance Spectroscopy setup. We would also like to thank the Material Characterization Laboratory (MCL) at Pennsylvania State University for help with the TEM. We acknowledge the financial support of ONR through award N00014-11-1-0665.

[1] R. M. Bowman and J. M. Gregg, J. Mater. Sci. **9**, 187 (1998); C. Ko, Z. Yang, and S. Ramanathan, ACS Appl. Mater. Interfaces **3**, 3396 (2011).
[2] L. L. Ladd and W. Paul, Solid State Commun. **7**, 425 (1969).
[3] G. Stefanovich, A. Pergament, and D. Stefanovich, J. Phys. Condens. Matter **12**, 8837 (2000).
[4] K. Okimura and J. Sakai, Jpn. J. Appl. Phys., Part 2 **46**, L813 (2007).
[5] B. G. Chae, H. T. Kim, D. H. Youn, and K. Y. Kang, Physica B **369**, 76 (2005).
[6] J. T. S. Irvine, D. C. Sinclair, and A. R. West, Adv. Mater. **2**, 132 (1990).
[7] H. Paik, J. Moyer, J. A. Mundy, J. Tashman, D. A. Muller, P. Schiffer, and D. G. Schlom, "Structure and transport property of ultrathin epitaxial VO_2 thin film on TiO_2 (001) substrate grown by MBE" (unpublished).
[8] J. R. Macdonald, Ann. Biomed. Eng. **20**, 289 (1992).
[9] R. Schmidt, W. Eerenstein, T. Winiecki, F. D. Morrison, and P. A. Midgley, Phys. Rev. B **75**, 245111 (2007).
[10] M. M. Qazilbash, M. Brehm, B.-G. Chae, P. C. Ho, G. O. Andreev, B.-J. Kim, S. J. Yun, A. V. Balatsky, M. B. Maple, F. Keilmann, H.-T. Kim, and D. N. Basov, Science **318**, 1750 (2007).
[11] S. Zhang, J. Y. Chou, and L. J. Lauhon, Nano Lett. **9**, 4527 (2009).
[12] J. F. Palmier and Y. Ballini, Solid State Commun. **14**, 575 (1974).
[13] A. Mansingh, R. Singh, and M. Sayer, J. Phys. Chem. Solids **45**, 79 (1984).
[14] J. B. Goodenough, J. Solid State Chem. **3**, 490 (1971).

This article is copyrighted as indicated in the article. Reuse of AIP content is subject to the terms at: http://scitation.aip.org/termsconditions. Downloaded to IP: 128.84.143.26 On: Mon, 27 Apr 2015 13:54:41